



Fermi National Accelerator Laboratory

FERMILAB-FN-576

Heavy Flavor Photoproduction Results from E687

presented by J. Wiss

*Fermi National Accelerator Laboratory
P.O. Box 500, Batavia, Illinois 60510*

for the E687 Collaboration

November 1991

Presented at the *Third Topical Seminar on Heavy Flavours*, San Miniato, Tuscany (Italy), June 17-21, 1991.



Disclaimer

This report was prepared as an account of work sponsored by an agency of the United States Government. Neither the United States Government nor any agency thereof, nor any of their employees, makes any warranty, express or implied, or assumes any legal liability or responsibility for the accuracy, completeness, or usefulness of any information, apparatus, product, or process disclosed, or represents that its use would not infringe privately owned rights. Reference herein to any specific commercial product, process, or service by trade name, trademark, manufacturer, or otherwise, does not necessarily constitute or imply its endorsement, recommendation, or favoring by the United States Government or any agency thereof. The views and opinions of authors expressed herein do not necessarily state or reflect those of the United States Government or any agency thereof.

Heavy Flavor Photoproduction Results from E687

Presented by Jim Wiss for the E687 Collaboration

Fermilab experiment E687 is a collaboration of ≈ 60 physicists representing primarily institutions in the United States and Italy⁽¹⁾.

E687 studies the photoproduction of charm particles using bremsstrahlung photons produced in an energy range from 100 to 400 GeV. The apparatus consists of a multiparticle magnetic spectrometer with excellent vertexing, particle identification, and calorimetric capabilities. The magnetic spectrometer, consisting of two analysis magnets interleaved with 5 MWPC stations (13,400 wires) provides 1.4% σ_p/p resolution for 100 GeV tracks traversing both analysis magnets, and 3.4% resolution for 100 GeV tracks traversing just the first magnet. The microstrip vertex detector, consisting 8,400, fully pulse height analyzed strips, provides $\sigma = 9 \mu\text{m}$ transverse extrapolation resolution for stiff tracks projected to the target plane. Smearing due to multiple coulomb scattering equals the momentum and vertex measurement errors at a momentum of ≈ 20 GeV. The typical charm proper time resolution is measured to be $\sigma_\tau \approx 0.048$ ps. Three threshold Cerenkov counters (with a total of 300 cells) allow kaons to be separated from lighter particles over a momentum range from 5 to 62 GeV. Electron identification is provided over the full instrumented solid angle by both an inner and outer electromagnetic calorimeter. Muon identification is provided by arrays of scintillation counters and proportional tubes in back of steel walls. The data on which the following talk is based was collected from December, 1987 to February, 1988 and consists of approximately 10,000 fully reconstructed charm particles. The electron beam endpoint and triggering conditions during this run produced data with an average photon energy of 220 GeV.

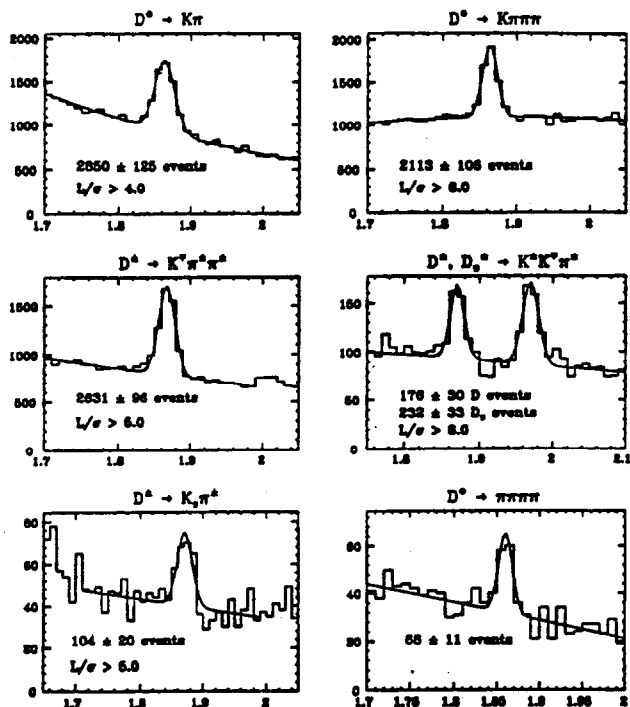
Lifetime tagging is the primary tool used in E687 to isolate charm particles from the very copious, photoproduced backgrounds. Two different approaches to the problem of finding primary and decay vertices

are used in E687. The "stand alone" vertex finder searches for events containing more than one cleanly isolated vertex by striving to build the highest multiplicity vertices with an acceptable χ^2 . The charm signals obtained with the stand alone vertex finder are very clean, but the algorithm is necessarily inefficient at short decay times. An alternative approach, the "candidate driven" vertex finder, searches for charm decays into specified decay modes. The charmed particle candidate is *assumed* to form a secondary vertex. A "seed" track which passes through the secondary vertex and is directed along the D candidate's momentum vector is used to search for the primary vertex by including tracks which form high confidence level intersections with the seed track. The efficiency of this algorithm in finding primary vertices is nearly independent of the vertex separation. Backgrounds are reduced in the candidate driven algorithm by making simultaneous cuts on the confidence level of the secondary vertex and on the statistical significance of vertex detachment (ℓ/σ) where ℓ is the distance between the primary and secondary vertex. Figure 1 shows some high statistics or interesting charm signals obtained in the 1987-1988 E687 run. The vertex detachment cut is noted on the figure when the signal is obtained via the candidate driven vertex finder.

1. Photoproduction Studies

High energy photoproduction is traditionally analyzed in terms of the photon-gluon fusion model in which a charm - anticharm quark pair is created which carries essentially all of the photon energy, and each quark carries $\langle P_\perp \rangle \approx 1$ GeV. The cross section grows slowly with increasing photon energy well above threshold.

FIG. 1



We measure inclusive charm / $\overline{\text{charm}}$ ratio's consistent with unity for the D^+ ($1.06 \pm .06$), the D^{*+} ($1.07 \pm .09$) and the Λ_c^+ ($.99 \pm .33$). No significant change in this ratio (measured for the D^+) is observed as a function of meson momentum. Deviation of charm / $\overline{\text{charm}}$ ratio from unity is a signature for asymmetric charm photoproduction mechanisms such as associated production. The D^+ inclusive P_{\perp} distribution is well fit to the form:

$$\frac{d\sigma}{dp_{\perp}^2} \propto e^{a_1 p_{\perp}^2 + a_2 p_{\perp}^4} \quad \text{where } a_1 = -.93 \pm .05 \text{ GeV}^{-2} \quad \text{and } a_2 = +.04 \pm .010 \text{ GeV}^{-4}$$

Both the charm / $\overline{\text{charm}}$ and P_{\perp} distributions are similar to those obtained⁽²⁾ by the E691 experiment at a mean energy of ≈ 120 GeV.

Naively, one expects that D^{*} 's and D 's are photoproduced proportional to the ratio of their available spin states or 3:1. Under this assumption, the additional assumption that $I_3 = \pm 1/2$ states are produced equally, and using the 1990 PDG branching ratios, one calculates that the ratio of observed $D^* \rightarrow D^0 \pi^+$

decays to observed inclusive D^0 decays should be $0.27 \pm .03$. We obtain the value $.24 \pm .013 \pm .01$ for this ratio; while E691⁽²⁾ obtained $.32 \pm .01 \pm .03$.

Figure 2 gives the $d\sigma/dX_f$ distributions obtained for the D^0 and D^+ mesons. The curve superimposed on the figures is the (arbitrarily scaled) parameterization obtained by E691⁽²⁾. It is worth noting that the average X_f value is considerably lower than 0.5 - the value expected in photon-gluon fusion in the absence of dressing effects.

Figure 3 compares our measurements of the total charm photoproduction cross section as a function of energy to other measurements (and to the next to leading order calculations of Ellis & Nason). Our values are deduced from $\sigma \cdot \text{BR}(X_f > 0)$ measured for the process $D^+ \rightarrow K^- \pi^+ \pi^+$ under the assumption of a linear A dependence, a branching fraction of 7.9 %,

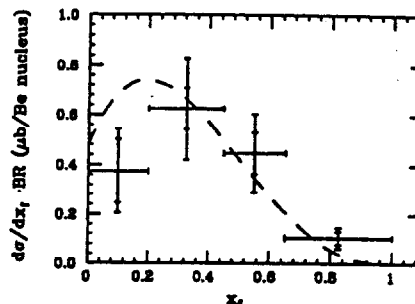


FIG. 2

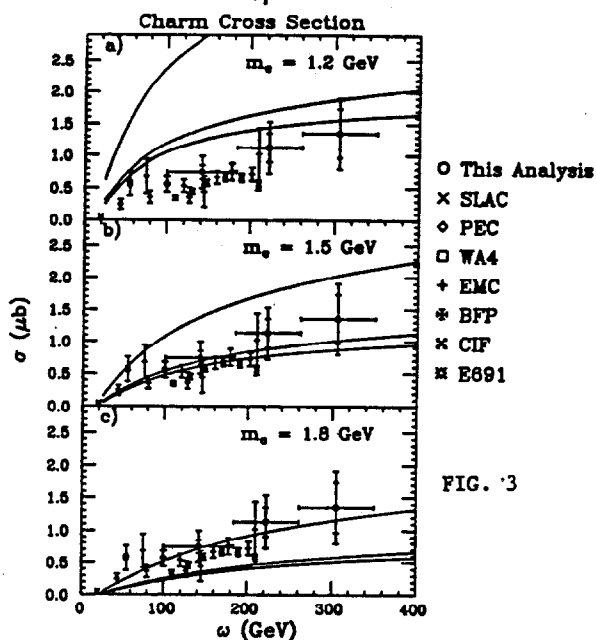


FIG. 3

and a factor of 2.42 to convert from the D^+ inclusive to charm total cross section. The cross section data shown in Figure 2 and 3 is corrected for the large ± 45 GeV uncertainty in primary beam energy through a deconvolution procedure. The beam energy uncertainty dominates the cross section error bars. In E687 data taken subsequent to the 87-88 data reported here primary beam energy uncertainty has been reduced to about ± 10 GeV through the use of a high rate microstrip beam tagging spectrometer.

All of the E687 photoproduction studies reported here are essentially consistent with the expectations of the photon-gluon fusion model.

2. Charm Particle Lifetimes

The E687 charm particle lifetime measurements⁽³⁾ are summarized in Table 1.

Table 1 -Lifetimes

	E687 τ (ps)	1990 PDG
D^0	$.424 \pm .011 \pm .007$	$.42 \pm .01$
D^+	$1.075 \pm .040 \pm .018$	$1.062 \pm .028$
D_s^+	$.50 \pm .06 \pm .03$	$.445 (+.035 - .029)$
Λ_c^+	$.20 \pm .03 \pm .03$	$.19 (+.017 - .013)$

I would like to briefly review the method used to determine the D^0 and D^+ lifetimes.

We use four independent samples for the D^0 consisting of $D^0 \rightarrow K \pi$ & $K3\pi$ samples and $D^{*+} \rightarrow D^0 \pi^+$ tag and no-tag samples. For each of these 4 disjoint samples we apply the minimum l/σ cuts which achieves a 1:1 signal to noise ratio which ranges from 0 for the $K\pi$ D^0 tag sample to 7 for the $K3\pi$. We use the $K^-\pi^+\pi^+$ decay mode with an $l/\sigma > 5$ cut to determine the lifetime of the D^+ . The resultant mass distributions which contain a total of about ≈ 7500 signal events are shown in Figure 4.

Separate lifetime estimates for the 4 D^0 samples and the D^+ sample were made with binned maximum likelihood technique using the *reduced* proper lifetime

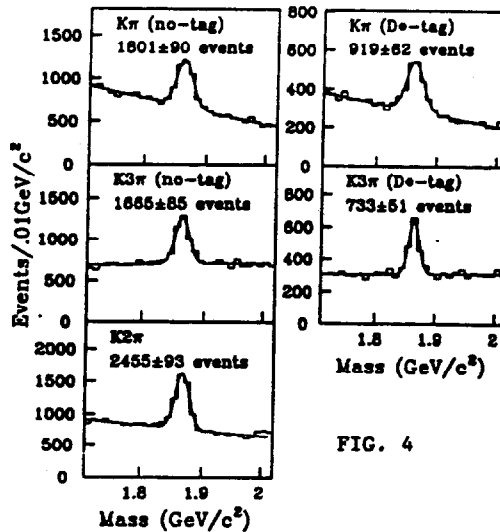


FIG. 4

variable: $t = t_{\text{meas}} - N \sigma_t$ where we subtract the required number of standard deviations of vertex detachment from the measured proper time between the primary and secondary vertices. Twenty-five bins spanning 6 nominal lifetimes are used where the anticipated number of events in a given time bin given by:

$$\mu_i = A f(t_i) e^{-t_i/\tau} + B b_i$$

In this expression τ is the charm lifetime fit parameter, b_i is the background lifetime shape (directly taken from events in the mass sidebands), B is the background level fit parameter, and $f(t_i)$ is a Monte Carlo deduced lifetime correction factor which incorporates resolution, geometrical, and absorption effects to the charm lifetime. The $f(t)$ function is very flat even at short reduced proper times owing to the use of the candidate driven vertex finder for the analysis and data skimming of the experiment.

The likelihood is the product of the Poisson probability that τ and B describe the lifetime evolution of signal region events and the Poisson probability that the level B matches the number of events in the two-mass sidebands.

$$\mathcal{L} = \prod \mathcal{P}(N_i, \mu_i) \times \mathcal{P}(N_{sb}, 2B)$$

The errors from the likelihood fit were increased slightly to account for additional statistical fluctuations in b_i and the estimates were adjusted for some

biases small in the fitting procedure discovered through extensive Monte Carlo simulation.

Figure 5 shows the results of the 5 separate lifetime fits over a wide range of ℓ/σ cuts. We quote the lifetimes which corresponds to the detachment cuts used for Figure 4. At these detachment cuts, the four independent D^0 lifetime estimates were found to be consistent with the same lifetime with a 24 % confidence level. An independent analysis using the stand alone vertex finder confirmed these results. Systematic errors are dominated by uncertainty in the absorption correction (collision length or absorption length) and in the choice of mass sideband for background.

3. Branching Ratios

The table below shows several preliminary relative branching ratios obtained in E687 and compares these

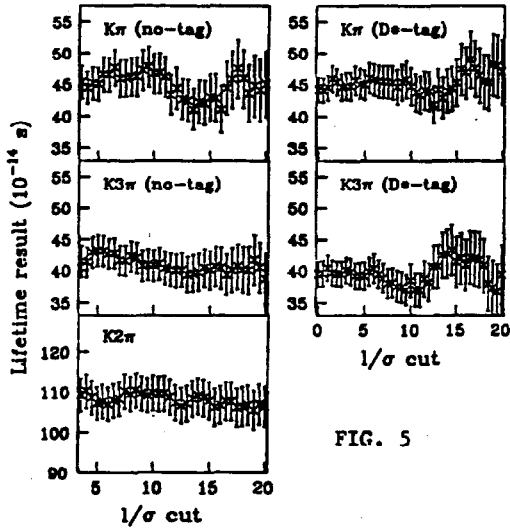


FIG. 5

values to either other experiments or compilations.

Some E687 signal yields are 68 ± 11 for 4π , 29 ± 9.3 for K^+K^- , 39 ± 8 for $K_s^+K^-$, and 21 ± 6.7 for $\phi 3\pi$. In order to reduce production model dependences relative branching ratios are obtained by fitting mass histograms where each event is weighted by $1/\epsilon(P)$ where $\epsilon(P)$ is the complete detection efficiency (reflecting geometrical, trigger, and analysis cuts) parameterized in terms of the charm particle lab momentum.

Several theoretical predictions exist for the $\Gamma(D^0 \rightarrow \bar{K}_s^0\phi)/\Gamma(D^0)$ branching ratio. This decay has been proposed by Bigi as a test of the importance of non-spectator contributions to charm decay. Our number from row 4 of the table when combined with the known $\bar{K}_s^0\pi^+\pi^-$ branching ratio implies $\Gamma(D^0 \rightarrow \bar{K}_s^0\phi)/\Gamma(D^0) = .77 \pm .37\%$ which is in good agreement with the prediction (.75 %) of the Bauer, Stech, and Wirbel⁽⁴⁾ factorization model, consistent with the prediction (1.3 %) of Block and Shifman⁽⁵⁾ QCD sum rule calculation but inconsistent with the $1/N$ expansion (0.15 %) prediction of Buras, Gerard, and Ruckl⁽⁶⁾.

4. Dalitz Plot Fits

The E687 collaboration is in the process of doing Dalitz plot analyses of the $D^+ \rightarrow K^- \pi^+ \pi^+$, $D^0 \rightarrow K_s^+ \pi^+ \pi^-$, and D_s^+ , $D^+ \rightarrow K^+ K^- \pi^+$ final states. A preliminary $D^0 \rightarrow K_s^+ \pi^+ \pi^-$ analysis will be discussed here. Two data samples were used in this analysis: (1) An inclusive sample, consisting of 195 signal events with a 1.3 S/N ratio after the imposition of an $\ell > 10\sigma$

Branching Ratios

		E687	Exp 1	Exp 2
D^0	$\pi^+\pi^-\pi^+\pi^-/K^-\pi^+\pi^-\pi^+$	$.10 \pm .02 \pm .02$	$.096 \pm .018 \pm .007^p$	$.102 \pm .013^c$
D^0	$K^+K^-/K^-\pi^+$	$.12 \pm .03$	$.119 \pm .018^p$	$.122 \pm .018 \pm .012^m$
D^0	$\bar{K}_s^0 K^+ K^- / \bar{K}_s^0 \pi^+ \pi^-$	$.198 \pm .057 \pm .078$	$.20 \pm .05^p$	$.170 \pm .022^a$
D^0	$\bar{K}_s^0 \phi / \bar{K}_s^0 \pi^+ \pi^-$	$.121 \pm .057 \pm .090$	$.155 \pm .033^a$	$.163 \pm .023^c$
D^0	$\bar{K}_s^0 (K^+ K^-)_{\text{non-}\phi} / \bar{K}_s^0 \pi^+ \pi^-$	$.136 \pm .042 \pm .068$	$.084 \pm .02^a$	$.12 \pm .032^p$
D_s^+	$\phi \pi^+ \pi^- \pi^+ / \phi \pi^+$	$.58 \pm .20 \pm .10$	$.42 \pm .13^p$	$1.11 \pm .37 \pm .28^a$

^a ARGUS ^c CLEO ^m MARK3 ^p E691 ^p Particle Data Group

cut and (2) A D^* tag sample which consisted of 69 events with a S/N of 3.2 after the imposition of mass difference and $\ell > 5\sigma$ cuts. A rather tight mass cut ($\pm 8\sigma$) is used to reduce the Dalitz background for the inclusive sample. Figure 6 gives the Dalitz scatter plot and mass projections for the inclusive sample. Clear $K^*(890)$ enhancements are observed in both $K_s \pi^\pm$ mass projections. The K^{*+} resonance, produced by \bar{D} decay, populates a vertical Dalitz band; while the K^{*-} from D decay populates a band along the "hypotenuse" of the Dalitz plot. A marked depopulation exists towards the center of each band since the K^* decay axis is distributed according to $\cos^2 \theta$ with respect to the pion produced against the K^* .

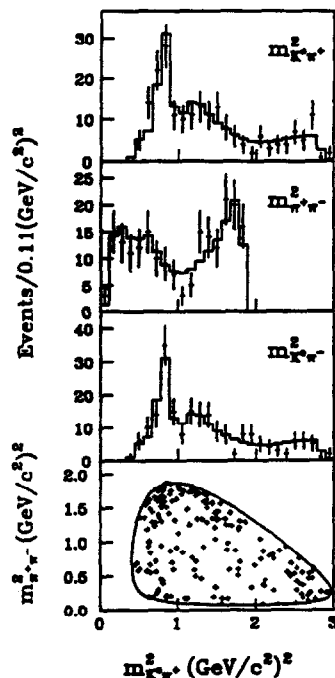


FIG. 6

The Dalitz plot was fit to a coherent amplitude which includes a K^* , ρ and non-resonant (phase space) contribution of the form:

$$\mathcal{A}(D) = a_1 e^{i\delta_1} + B(K_s \pi^- \pi^+ | K^*) + a_3 e^{i\delta_3} B(\pi^+ \pi^- K_s | \rho)$$

Here B represents p-wave Breit-Wigner amplitudes (and spin factors) for a resonance of mass M_r and width Γ of the form:

$$B(a b c | r) = -2 \vec{c} \cdot \vec{a} \frac{\sqrt{M_r \Gamma}}{M_r^2 - M_{ab}^2 - i \Gamma M_r}, \quad \Gamma \propto P_*^3$$

The \vec{c} and \vec{a} are the three momenta of particles a and c measured in the ab cm frame. The four fit parameters represent the (complex) coefficient of the non-resonant amplitude with respect to the K^* ($a_1 \exp(i\delta_1)$) and the ρ amplitude with respect to the K^* ($a_3 \exp(i\delta_3)$). The Dalitz density is fit to the average of the intensities for the D and \bar{D} where the $\mathcal{A}(\bar{D})$ is obtained from the $\mathcal{A}(D)$ through the exchange $\pi^\pm \rightarrow \pi^\mp$. A background contribution is included which was obtained from a fit to the mass sidebands.

The preliminary, fitted a_1 and a_3 values imply equal fractions of about 14 % for the non-resonant and ρK_s decay, and about 81 % for the $K^* \pi$ decay. The fraction for a given contribution is obtained by setting all other contributions to zero, integrating over the full Dalitz plot, and dividing by the integral with all three contributions present. Both the δ_1 and δ_3 phases were close to -1.75 radians. The lower statistics but cleaner D^* tag sample fits are consistent with these values.

4. The Future

Severe time and space limitations have prevented me from reviewing new results of E687 on D^+ semileptonic decays, D_s^+ semileptonic decays charm baryon branching ratios, Ψ photoproduction, and new limits on $D - \bar{D}$ mixing. We have accumulated about 5 times the 1987-1988 data sample reported here in 1990 and are presently engaged in a 1991 run where we hope to bring our total data sample up to a factor of 9 times the data reported here.

1. E687 institutions include Milan, Frascati, Pavia, Bologna from Italy. Colorado, Fermilab, Illinois, Northwestern, UC Davis, from the United States.
2. Anjos et al., PRL 62:513 (1989)
3. Frabetti et al., Phys. Lett. B251:639 (1990) & Frabetti et al., Phys. Lett. B263:584 (1991)
4. Bauer, Stech, Phys. Lett. 152B:380 (1985)
5. Buras, Gerard, Ruckl, Nucl. Phys. B268: 16 (1986)
6. Blok, Shifman, Soviet Journal Nucl Phys. 45, 135 (1987)